

Synthesis, Structure, and Properties of the Noncentrosymmetric Hydrated Borate $\text{Na}_2\text{B}_5\text{O}_8(\text{OH}) \cdot 2\text{H}_2\text{O}$

Yongjiang Wang,^{†,‡} Shilie Pan,^{*,†} Xuelin Tian,[†] Zhongxiang Zhou,[†] Gang Liu,[§] Jide Wang,[§] and Dianzeng Jia[§]

[†]Xinjiang Key Laboratory of Electronic Information Materials and Devices, Xinjiang Technical Institute of Physics & Chemistry, Chinese Academy of Sciences, 40-1 South Beijing Road, Urumqi 830011, China,

[‡]Graduate School of the Chinese Academy of Sciences, Beijing 100039, China, and [§]College of Chemistry and Chemical Engineering, Xinjiang University, Urumqi 830046, China

Received April 9, 2009

Single crystal of hydrated sodium borate $\text{Na}_2\text{B}_5\text{O}_8(\text{OH}) \cdot 2\text{H}_2\text{O}$ has been grown with sizes up to $5 \times 5 \times 3 \text{ mm}^3$ under mild hydrothermal conditions at 180 °C. The structure is determined by single-crystal X-ray diffraction and further characterized by IR and TG analyses. It crystallizes in the orthorhombic space group $Pna2_1$, with $a = 11.967(2) \text{ \AA}$, $b = 6.5320(13) \text{ \AA}$, $c = 11.126(2) \text{ \AA}$, $Z = 4$, $R1 = 0.0183$, and $wR2 = 0.0483$. The crystal structure of $\text{Na}_2\text{B}_5\text{O}_8(\text{OH}) \cdot 2\text{H}_2\text{O}$ is made up of Na–O polyhedra, and $[\text{B}_5\text{O}_8(\text{OH})]^{2-}$ polyborate anions. Transmittance spectrum is performed on the $\text{Na}_2\text{B}_5\text{O}_8(\text{OH}) \cdot 2\text{H}_2\text{O}$ crystal, which shows an absorption edge less than 190 nm in the UV region. The powder second-harmonic generation intensity measured by the Kurtz–Perry method indicates that $\text{Na}_2\text{B}_5\text{O}_8(\text{OH}) \cdot 2\text{H}_2\text{O}$ is about half that of KH_2PO_4 (KDP).

Introduction

Noncentrosymmetric (NCS) compounds are of current interest in materials chemistry owing to their important properties such as second-harmonic generation (SHG), ferroelectricity, piezoelectricity, and pyroelectricity.^{1–3} Recently, a variety of strategies have been put forth for the design of new NCS materials, and there has been considerable progress in the development of coherent sources based on NCS processes

in borate crystals.^{4–10} The success of these crystals can be attributed to the unique structural characteristics of boron–oxygen group, with planar BO_3 and tetrahedral BO_4 groups as the basic structures, and these BO_3 triangles and BO_4 tetrahedra can further link together via common oxygen atoms to form isolated rings and cages or polymerize into infinite chains, sheets, and networks. We have chosen to investigate the borate system, especially alkali metal and alkaline earth metal borates, which have produced a large family of compounds with outstanding physical properties, such as $\beta\text{-BaB}_2\text{O}_4$, LiB_3O_5 , and $\text{KBe}_2\text{BO}_3\text{F}_2$.¹¹ Though more and more new deep-UV nonlinear optical (NLO) materials have been discovered, these NLO materials have their own drawbacks that limit their applications. Therefore, the research of other new NLO materials is still needed. Our investigation of the alkali metal borate system resulted in the finding of noncentrosymmetric materials, $\text{Na}_2\text{B}_5\text{O}_8(\text{OH}) \cdot 2\text{H}_2\text{O}$.

The $\text{Na}_2\text{B}_5\text{O}_8(\text{OH}) \cdot 2\text{H}_2\text{O}$ compound was first reported with space group $Pna2_1$ by Corazza et al. in 1975.¹² The $\text{Na}_4[\text{B}_{10}\text{O}_{16}(\text{OH})_2] \cdot 4\text{H}_2\text{O}$ compound was reported to crystallize in the monoclinic space group Pc by Liu et al. in 2006.¹³ It is noteworthy that there are different space groups in these

*To whom correspondence should be addressed. Phone: (86)991-3674558. Fax: (86)991-3838957. E-mail: slpan@ms.xjb.ac.cn.

- (1) (a) Chen, C. T.; Liu, G. Z. *Annu. Rev. Mater. Sci.* **1986**, *16*, 203.
- (b) Goody, J.; Broussard, J.; Halasyamani, P. S. *Chem. Mater.* **2002**, *14*, 3174.
- (c) Halasyamani, P. S.; Poeppelmeier, K. R. *Chem. Mater.* **1998**, *10*(10), 2753.
- (2) (a) Lang, S. B. *Phys. Today* **2005**, *58*, 31. (b) Lin, X. S.; Zhang, G.; Ye, N. *Cryst. Growth Des.* **2009**, *9*(2), 1186. (c) Chen, C. T.; Ye, N.; Lin, J.; Jiang, J.; Zeng, W. *Adv. Mater.* **1999**, *11*, 1071.
- (3) (a) Becker, P. *Adv. Mater.* **1998**, *10*, 979. (b) Auciello, O.; Scott, J. F.; Ramesh, R. *Phys. Today* **1998**, *51*, 22. (c) Galy, J.; Meunier, G. *J. Solid State Chem.* **1975**, *13*, 142. (d) Jona, F.; Shirane, G. *Ferroelectric Crystals*; Pergamon Press: Oxford, U. K., 1962.
- (4) (a) Zyss, J.; Oudar, J. L. *Phys. Rev. A* **1982**, *26*, 2028. (b) Halasyamani, P. S.; O'Hare, D. *Chem. Mater.* **1998**, *10*, 646. (c) Hagerman, M. E.; Poeppelmeier, K. R. *Chem. Mater.* **1995**, *7*(4), 602.
- (5) (a) Mao, J. G.; Jiang, H. L.; Fang, K. *Inorg. Chem.* **2008**, *47*, 8498. (b) Pan, S. L.; Wu, Y. C.; Fu, P. Z.; Zhang, G. C.; Li, Z. H.; Du, C. X.; Chen, C. T. *Chem. Mater.* **2003**, *15*, 2218. (c) Pan, S. L.; Smit, J. P.; Watkins, B.; Marvel, M. R.; Stern, C. L.; Poeppelmeier, K. R. *J. Am. Soc. Chem.* **2006**, *128*, 11631. (d) Muller, E. A.; Cannon, R. J.; Sarjeant, A. N.; Ok, K. M.; Halasyamani, P. S.; Norquist, A. *Cryst. Growth Des.* **2005**, *5*(5), 1913.
- (6) Marder, S. R.; Beratan, D. N.; Cheng, L. T. *Science* **1991**, *252*, 103.
- (7) Wu, Y. C.; Sasaki, T.; Nakai, S.; Yokotani, A.; Tang, H. G.; Chen, C. T. *Appl. Phys. Lett.* **1993**, *62*, 2614.
- (8) Grice, J. D.; Burns, P. C.; Hawthorne, F. C. *Can. Mineral.* **1999**, *37*, 731. (b) Burns, P. C.; Grice, J. D.; Hawthorne, F. C. *Can. Mineral.* **1995**, *33*, 1131. (c) Cannillo, E.; Dal Negro, A.; Ungaretti, L. *Am. Mineral.* **1973**, *58*, 110.

- (9) Liu, Y. S.; Dentz, D.; Belt, R. *Opt. Lett.* **1983**, *9*, 76.
- (10) Kato, K. J. *IEEE J. Quantum Electron.* **1986**, *31*, 169.
- (11) (a) Chen, C. T.; Wu, B. C.; Jiang, A. D.; You, G. M. *Sci. Sin.* **1985**, *B18*, 235. (b) Chen, C. T.; Wu, Y. C.; Jiang, A.; You, G.; Li, R.; Lin, S. J. *Opt. Soc. Am.* **1989**, *B6*, 616. (c) Wang, G. L.; Zhou, Y.; Li, C. M.; Xu, Z. Y.; Wang, X. Y.; Zhu, Y.; Chen, C. T. *Appl. Phys.* **2008**, *B91*, 95.
- (12) Corazza, E.; Menchetti, S.; Sabelli, C. *Acta Crystallogr.* **1975**, *31*, 2405.
- (13) Liu, Z. H.; Li, L. Q.; Wang, M. Z. *J. Alloys Compd.* **2006**, *407*, 334.

studies.^{12,13} To our knowledge, both of these investigations were focused on the synthesis, the studies of the second-order NLO properties have not been reported. Apart from that, further understanding of the relationship between the structure and the properties of these compounds prompts us to reinvestigate the crystal structure using the single-crystal X-ray diffraction, which permits us to establish with certainty the existence and formula of a compound. The present paper reports the synthesis, structure, and characterization of $\text{Na}_2\text{B}_5\text{O}_8(\text{OH})\cdot 2\text{H}_2\text{O}$ crystal.

Experimental Section

Reagents. $\text{Na}_2\text{B}_4\text{O}_7\cdot 10\text{H}_2\text{O}$ (Tianjin Bodi Chemical Co., Ltd., 99.5%), NaOH (Tianjin Bodi Chemical Co., Ltd., 99.5%), and H_3BO_3 (Tianjin Baishi Chemical Co., Ltd., 99.5%) were used as received.

Synthesis. For $\text{Na}_2\text{B}_5\text{O}_8(\text{OH})\cdot 2\text{H}_2\text{O}$, 3.814 g (1.00×10^{-2} mol) of $\text{Na}_2\text{B}_4\text{O}_7\cdot 10\text{H}_2\text{O}$ and 1.8554 g (3.00×10^{-2} mol) of H_3BO_3 were combined with 0.5 mL of H_2O . The solution was placed in a 23 mL Teflon-lined autoclave that was subsequently sealed. The autoclave was heated to 180 °C gradually, held for 3 days, and cooled to room temperature for 9 days. The crystal was obtained in the autoclave. The resulting colorless and transparent crystals could easily be separated from the solution by filtration and washed with deionized water for the reported crystal is insoluble in cold water.

Powder X-ray Diffraction. Powder X-ray diffraction was performed on an automated Bruker D8 ADVANCE X-ray diffractometer equipped with a diffracted-beamed monochromatic set for Cu K α ($\lambda = 1.5418$ Å) radiation and a nickel filter at room temperature in the angular range from 10 to 70° (2θ) with a scanning step width of 0.02° and a fixed counting time of 1 s/step.

X-ray Crystallographic Studies. A colorless and transparent crystal of $\text{Na}_2\text{B}_5\text{O}_8(\text{OH})\cdot 2\text{H}_2\text{O}$ with the dimension $0.59 \times 0.40 \times 0.40$ mm³ was chosen for the structure determination. Unit cell parameters were derived from a least-squares analysis of 2502 reflections in the range of $3.40^\circ < \theta < 27.47^\circ$. Intensity data were collected on a Rigaku R-axis Spider using graphite-monochromated Mo K α radiation ($\lambda = 0.71073$ Å) and integrated with the SAINT-Plus program.¹⁴ All calculations were performed with the SHELXTL-97 crystallographic software package.¹⁵ Final least-squares refinement on F_0^2 with data having $F_0^2 \geq 2\sigma(F_0^2)$ includes anisotropic displacement parameters for non-hydrogen atoms. The final difference Fourier synthesis may have shown maximum and minimum peaks at 0.166 and -0.192 e/Å³, respectively.

The structures were checked for missing symmetry elements with PLATON.¹⁶ Crystal data and structure refinement information are summarized in Table 1. Final atomic coordinates and equivalent isotropic displacement parameters of the title compound are listed in Table S1a in the Supporting Information. Selected interatomic distances and angles are given in Tables S1b and c in the Supporting Information.

Infrared Spectroscopy. The infrared spectroscopy was recorded on a Bruker Equinox 55 Fourier transform infrared spectrometer. The spectrum was collected using the $\text{Na}_2\text{B}_5\text{O}_8(\text{OH})\cdot 2\text{H}_2\text{O}$ crystal in the range from 600 to 4000 cm⁻¹ with a resolution of 2 cm⁻¹.

Thermal Analysis. The thermal analyses were carried out on a simultaneous Netzsch STA 449C thermal analyzer instrument,

Table 1. Crystal Data and Structure Refinement for $\text{Na}_2\text{B}_5\text{O}_8(\text{OH})\cdot 2\text{H}_2\text{O}$

empirical formula	$\text{Na}_2\text{B}_5\text{O}_8(\text{OH})\cdot 2\text{H}_2\text{O}$
formula weight	281.07
temperature	153(2) K
wavelength	0.71073 Å
crystal system	orthorhombic
space group	$Pna2_1$
unit cell dimensions	$a = 11.967(2)$ Å, $\alpha = 90^\circ$ $b = 6.5320(13)$ Å, $\beta = 90^\circ$ $c = 11.126(2)$ Å, $\gamma = 90^\circ$
volume	$869.7(3)$ Å ³
Z	4
density (calculated)	2.146 g/cm ³
absorption coefficient	0.288 mm ⁻¹
$F(000)$	560
crystal size	$0.59 \times 0.56 \times 0.40$ mm ³
θ range for data collection	$3.40\text{--}27.47^\circ$
limiting indices	$-15 \leq h \leq 15$ $-8 \leq k \leq 8$ $-13 \leq l \leq 14$
reflections collected	8015/1914 [$R_{\text{int}} = 0.0214$]
completeness to $\theta = 7.47^\circ$	99.8%
refinement method	full-matrix least-squares on F^2
data/restraints/parameters	1914/1/184
goodness-of-fit on F^2	1.127
final R indices [$I > 2\sigma(I)$] ^a	R1 = 0.0183, wR2 = 0.0483
R indices (all data)	R1 = 0.0185, wR2 = 0.0485
absolute structure parameter	$-0.07(19)$
extinction coefficient	0.066(3)
largest diff. peak and hole	0.166 and -0.192 e Å ⁻³

^a $R1 = \sum ||F_o| - |F_c|| / \sum |F_o|$ and $wR2 = [\sum w(F_o^2 - F_c^2)^2 / \sum wF_o^4]^{1/2}$ for $F_o^2 > 2\sigma(F_o^2)$.

with a heating rate of 10 °C min⁻¹ in an atmosphere of flowing N₂ from 25 to 700 °C.

Elemental Analysis. For $\text{Na}_2\text{B}_5\text{O}_8(\text{OH})\cdot 2\text{H}_2\text{O}$, the elemental analyses (H) were determined on a PE-2400 element analyzer. The summary of ICP elemental analysis of Na and B was performed using a Varian Vita-Pro CCD Simultaneous ICP-OES spectrometer. Anal. Calcd for the $\text{Na}_2\text{B}_5\text{O}_8(\text{OH})\cdot 2\text{H}_2\text{O}$: H, 1.78; Na, 16.37; B, 19.23; Found: H, 1.76; Na, 16.36; B, 19.26.

UV-vis Transmission Spectrum. UV-vis transmission spectrum data for $\text{Na}_2\text{B}_5\text{O}_8(\text{OH})\cdot 2\text{H}_2\text{O}$ crystal sample were collected with a TU-1901 UV-vis-NIR spectrophotometer at room temperature, which can operate over the range 190–900 nm.

Nonlinear Optical Measurements. Powder SHG tests were carried out by the Kurtz–Perry method.¹⁷ Microcrystalline KDP served as the standard. About 120 mg of powder was pressed into a pellet, which was then irradiated with a pulsed infrared beam (10 ns, 10 kHz) produced by a Q-switched Nd:YAG laser of wavelength 1064 nm. A 532 nm filter was used to absorb the fundamental beam and pass the visible light onto a photomultiplier. A combination of a half-wave achromatic retarder and a polarizer was used to control the intensity of the incident power, which was measured with an identical photomultiplier connected to the same high-voltage source. This procedure was then repeated using a standard NLO material, in this case microcrystalline KDP, and the ratio of the second harmonic intensity outputs was calculated. Since the SHG efficiency has been shown to depend strongly on particle size,¹⁷ the $\text{Na}_2\text{B}_5\text{O}_8(\text{OH})\cdot 2\text{H}_2\text{O}$ crystal was ground and sieved into distinct particle size ranges, <20, 20–38, 38–55, 55–88, 88–105, 105–150, and 150–200 μm.

Results and Discussions

Synthesis and Growth. $\text{Na}_2\text{B}_5\text{O}_8(\text{OH})\cdot 2\text{H}_2\text{O}$. During the synthesis of the compound, the different initial

(14) SAINT-Plus, version 6.02A; Bruker Analytical X-ray Instruments, Inc.: Madison, WI, 2000.

(15) Sheldrick, G. M. SHELXTL, version 6.14; Bruker Analytical X-ray Instruments, Inc.: Madison, WI, 2003.

(16) Spek, A. L. *J. Appl. Crystallogr.* **2003**, *36*, 7.

(17) (a) Kurtz, S. Q.; Perry, T. T. *J. Appl. Phys.* **1968**, *39*, 3798.

(b) Dougherty, J. P.; Kurtz, S. K. *J. Appl. Crystallogr.* **1976**, *9*, 145.

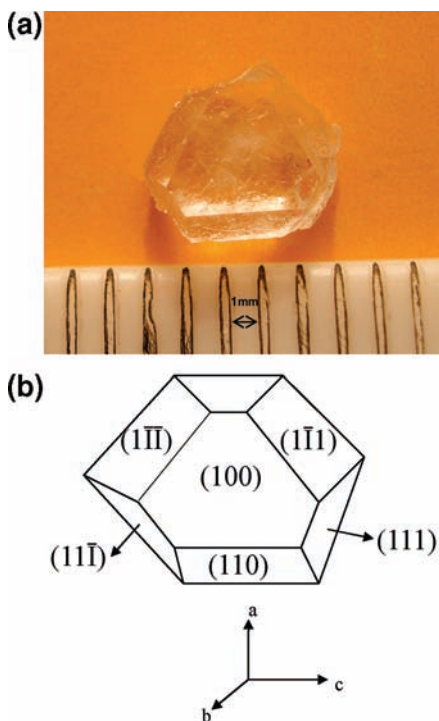


Figure 1. (a) Photograph of $\text{Na}_2\text{B}_5\text{O}_8(\text{OH})\cdot 2\text{H}_2\text{O}$ crystal. (b) Schematic representation and face indices of a $\text{Na}_2\text{B}_5\text{O}_8(\text{OH})\cdot 2\text{H}_2\text{O}$ crystal.

reagents and reaction ratio were attempted. When the initial reagents and reaction ratio were changed, another compound, $\text{Na}_2\text{B}_4\text{O}_5(\text{OH})_4\cdot 3\text{H}_2\text{O}$, was obtained.¹⁸ Therefore, the suitable reaction condition was used and the desired $\text{Na}_2\text{B}_5\text{O}_8(\text{OH})\cdot 2\text{H}_2\text{O}$ crystal with sizes up to $5 \times 5 \times 3 \text{ mm}^3$ was obtained. The yield based on Na is 96%. The photograph of the $\text{Na}_2\text{B}_5\text{O}_8(\text{OH})\cdot 2\text{H}_2\text{O}$ crystal with smooth faces is shown in Figure 1a, and the experimental powder X-ray diffraction pattern of $\text{Na}_2\text{B}_5\text{O}_8(\text{OH})\cdot 2\text{H}_2\text{O}$ crystal is in agreement with the calculated one based on the single-crystal data, which shows that the obtained sample is pure (see Figure S1a in the Supporting Information). The as-grown $\text{Na}_2\text{B}_5\text{O}_8(\text{OH})\cdot 2\text{H}_2\text{O}$ crystal was bounded by a combination of well-developed (100), (111), ($\bar{1}\bar{1}\bar{1}$), ($\bar{1}\bar{1}\bar{1}$), ($\bar{1}\bar{1}\bar{1}$) and (110) faces. Figure 1b shows the schematic representation and face indices of the crystal.

Structures. The crystal structure of $\text{Na}_2\text{B}_5\text{O}_8(\text{OH})\cdot 2\text{H}_2\text{O}$ is build up of Na–O polyhedra and $[\text{B}_5\text{O}_8(\text{OH})]^{2-}$ polyborate anions. According to the classification of polyborate anions proposed by Burns, Grice,

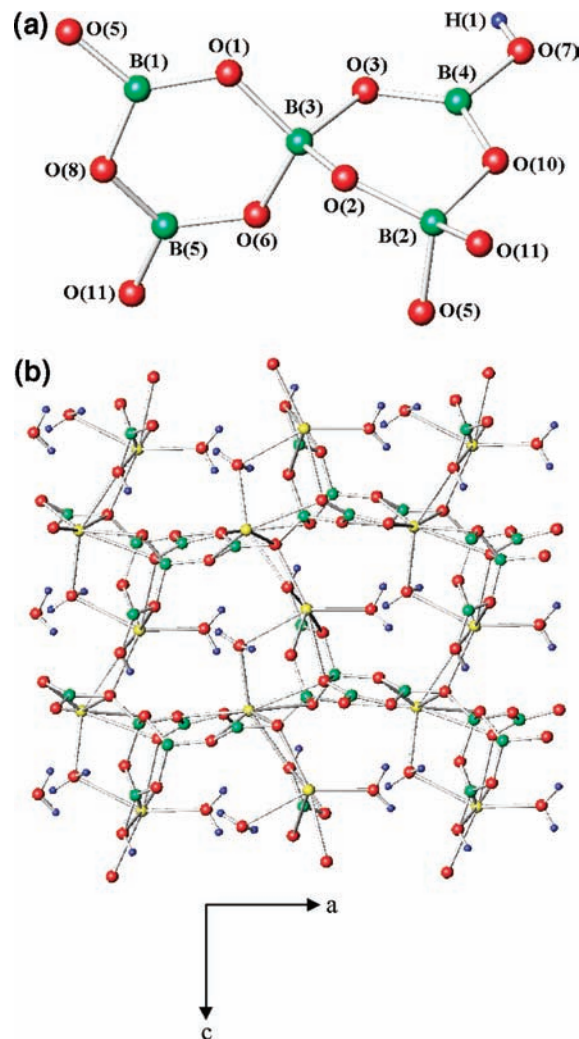


Figure 2. (a) Polyborate anion $[\text{B}_5\text{O}_8(\text{OH})]^{2-}$. (b) The packing diagram of $\text{Na}_2\text{B}_5\text{O}_8(\text{OH})\cdot 2\text{H}_2\text{O}$. The yellow spheres are Na, the green spheres are B, the red spheres are O, and the blue spheres are H.

and Hawthorne,⁸ the fundamental building blocks (FBBs) shorthand notation for $[\text{B}_5\text{O}_8(\text{OH})]^{2-}$ in $\text{Na}_2\text{B}_5\text{O}_8(\text{OH})\cdot 2\text{H}_2\text{O}$ is $3\Delta 2\Box: < 2\Delta\Box > - < \Delta 2\Box >$, the symbol of the descriptor gives the number of BO_3 triangles (Δ) and BO_4 tetrahedra (\Box) in the form $m\Delta n\Box$, where m and n are integers representing the number of BO_3 triangles and BO_4 tetrahedra. The polyion in $\text{Na}_2\text{B}_5\text{O}_8(\text{OH})\cdot 2\text{H}_2\text{O}$ has the same shape as the one found in ezcurrite $\text{Na}_4[\text{B}_5\text{O}_7(\text{OH})_3]_2\cdot 4\text{H}_2\text{O}$,⁸ with three triangles and two tetrahedra in the shape of a double hexagonal ring, which is almost perpendicular to each other, the two six-membered B–O normal-ring FBBs share one borate tetrahedron in the center (see Figure 2a). However, the basic $3\Delta 2\Box: < 2\Delta\Box > - < \Delta 2\Box >$ FBBs in $\text{Na}_2\text{B}_5\text{O}_8(\text{OH})\cdot 2\text{H}_2\text{O}$ links to form a sheet by sharing two triangle vertices with two tetrahedron vertices of neighboring FBBs and two tetrahedron vertices with two triangle vertices of neighboring FBBs. In ezcurrite, the FBBs shares two vertices between tetrahedra and triangles of adjacent clusters to form a chain.⁸

In $\text{Na}_2\text{B}_5\text{O}_8(\text{OH})\cdot 2\text{H}_2\text{O}$, the mean B–O distances of the BO_3 and BO_4 groups are 1.3685(14) and 1.4746(14) Å, respectively. The Na(1) atom is surrounded by eight O atoms, in which the Na–O distances range from

(18) During the process of synthesizing $\text{Na}_2\text{B}_5\text{O}_8(\text{OH})\cdot 2\text{H}_2\text{O}$, when the reagents and initial chemical ratio were changed, another crystal $\text{Na}_2\text{B}_4\text{O}_5(\text{OH})_4\cdot 3\text{H}_2\text{O}$ was obtained, which was reported by Carmelo et al (Carmelo, G.; Silivo, M.; Fernando, S. *Am. Mineral.* **1973**, *58*, 523). The detailed information is as follows: 0.8013 g (2.00×10^{-2} mol) of NaOH and 3.7099 g (6.00×10^{-2} mol) of H_3BO_3 were combined with 1 mL of H_2O in Teflon-lined autoclave. The autoclave was heated to 180 °C gradually, held for 2 days, and cooled to room temperature for 3 days. The crystal with sizes up to $6 \times 5 \times 4 \text{ mm}^3$ was obtained in the autoclave. The photograph of $\text{Na}_2\text{B}_4\text{O}_5(\text{OH})_4\cdot 3\text{H}_2\text{O}$ crystal is shown in Figure S2a in the Supporting Information, and the crystal purity was verified using X-ray diffraction, shown in Figure S2b in the Supporting Information. Its crystal data and structure refinement information are summarized in Table S2a in the Supporting Information. Final atomic coordinates and equivalent isotropic displacement parameters of the compound are listed in Table S2b in the Supporting Information. Selected interatomic distances and angles are given in Tables S2c and d in the Supporting Information.

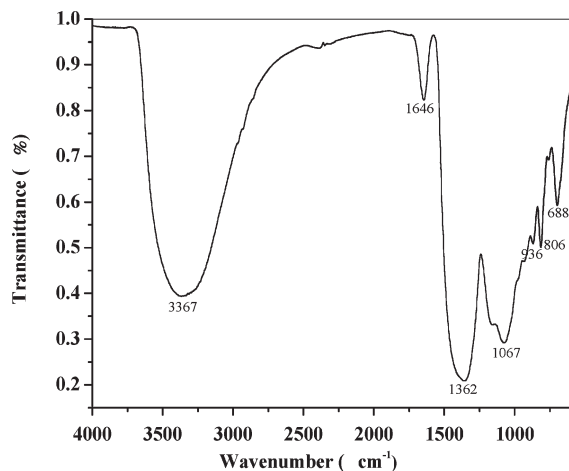


Figure 3. IR spectrum of the $\text{Na}_2\text{B}_5\text{O}_8(\text{OH})\cdot 2\text{H}_2\text{O}$ crystal.

2.3781(13) to 2.9717(12) Å. The Na(2) atom exhibits a 7-fold coordination, in which the Na–O distances range from 2.3518(11) to 2.8543(10) Å. There are two water molecules and one O–H in $\text{Na}_2\text{B}_5\text{O}_8(\text{OH})\cdot 2\text{H}_2\text{O}$.

The bonds between adjacent sheets in $\text{Na}_2\text{B}_5\text{O}_8(\text{OH})\cdot 2\text{H}_2\text{O}$ take place via H-bonding interaction and the Na polyhedra to form three-dimensional structure, with channels along the *b*-axis (see Figure 2b). Na^+ and H_2O as the forms of Na–O polyhedra are located in the channel and interact with the framework both electrostatically and via H-bonding.

Infrared Spectroscopy. Seen from Figure 3, the characteristic peaks of the $\text{Na}_2\text{B}_5\text{O}_8(\text{OH})\cdot 2\text{H}_2\text{O}$ crystal can be described as follows: The band at 3367 cm^{-1} is the stretching mode of O–H. The band at 1646 cm^{-1} is assigned to the H–O–H bending mode, which shows that the compound contains water molecules. The absorption peaks in IR spectrum of the synthetic sample were assigned on the basis of results obtained from vibrational spectra measurements of other borate group.¹⁹ The bands at 1362 and 936 cm^{-1} are the asymmetric stretching and symmetric stretching of B–O in BO_3 , respectively. The bands at 1067 and 806 cm^{-1} are likely the asymmetric and symmetric stretching of B–O in BO_4 , respectively. The bands at 688 cm^{-1} is the out-of-plane bending of B–O in BO_3 . Obviously, the $\text{Na}_2\text{B}_5\text{O}_8(\text{OH})\cdot 2\text{H}_2\text{O}$ crystal contains characteristic O–H, BO_3 , and BO_4 groups as its basic structural units, which is consistent with the above crystal structure results.

TG Analysis. The thermal behavior of $\text{Na}_2\text{B}_5\text{O}_8(\text{OH})\cdot 2\text{H}_2\text{O}$ is shown in Figure 4. TG analysis curve shows that the compound has three steps weight loss between 25 and $700\text{ }^\circ\text{C}$. The first weight loss is 6.48%, occurring from 25 to $250\text{ }^\circ\text{C}$, which corresponds to the loss of one crystal water molecule and can be compared with the calculated value of 6.40%. The weight loss in the second stage is 6.42%, from 250 to $390\text{ }^\circ\text{C}$, which corresponds to the loss of one crystal water molecule and can be compared with the calculated value of 6.40%. The

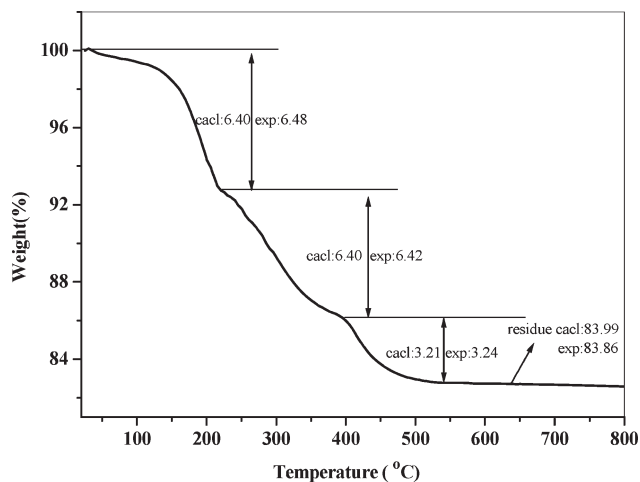


Figure 4. TG analysis curve of $\text{Na}_2\text{B}_5\text{O}_8(\text{OH})\cdot 2\text{H}_2\text{O}$.

weight loss in the last stage (found 3.24%, calcd 3.21%) from 390 to $700\text{ }^\circ\text{C}$ corresponds to the loss of 0.5 structural water molecules. The total weight loss is 16.14%, which corresponds to the loss of 2.5 water molecules and can be compared with calculated value of 16.01%.

UV–vis Transmission Spectroscopy. The transmission spectrum for $\text{Na}_2\text{B}_5\text{O}_8(\text{OH})\cdot 2\text{H}_2\text{O}$ crystal is shown in Figure S1b in the Supporting Information. It can be seen that a wide transmission range is observed with the UV absorption edge much less than 190 nm (a 70% transmission level at 190 nm). There are no absorption peaks in the whole range of the spectrum.

NLO Measurements. A simple and quick experimental technique is used to estimate the NLO effect and phase matching properties before the effect is made to grow large single crystals, which only requires the material in powder form and is named as the Kurtz–Perry method.¹⁷

On the basis of noncentrosymmetric crystal structures of $\text{Na}_2\text{B}_5\text{O}_8(\text{OH})\cdot 2\text{H}_2\text{O}$ and another hydrated borate $\text{Na}_2\text{B}_4\text{O}_5(\text{OH})_4\cdot 3\text{H}_2\text{O}$ synthesized by us,¹⁸ it is expected to possess NLO properties for them. According to the anionic group theory of NLO activity in borates,²⁰ the planar BO_3 groups and the nonplanar tetrahedral BO_4 groups would contribute to the SHG efficiency, and the latter contribute less. However, the different orientations of the structure limit their total NLO contribution. As a result, the overall SHG efficiency of $\text{Na}_2\text{B}_5\text{O}_8(\text{OH})\cdot 2\text{H}_2\text{O}$ remains moderate. This was confirmed by measuring its efficiency for SHG.

For $\text{Na}_2\text{B}_5\text{O}_8(\text{OH})\cdot 2\text{H}_2\text{O}$, Figure 5a gives the curves of SHG signal as a function of particle size from the measurements made on ground $\text{Na}_2\text{B}_5\text{O}_8(\text{OH})\cdot 2\text{H}_2\text{O}$ crystals. As the particle size of $\text{Na}_2\text{B}_5\text{O}_8(\text{OH})\cdot 2\text{H}_2\text{O}$ becomes significantly larger than its coherence length, the SHG intensity is independent of particle sizes. It was consistent with the phase-matching behavior according to the rules proposed by Kurtz and Perry,¹⁷ and $\text{Na}_2\text{B}_5\text{O}_8(\text{OH})\cdot 2\text{H}_2\text{O}$ was found to have a powder SHG effect about half times that of KDP. Furthermore, moderate green-light output was observed when 1064 nm-laser permeated the crystal along a special direction. All of

(19) (a) Wu, L.; Zhang, Y.; Chen, X. L.; Kong, Y. F.; Sun, T. Q.; Xu, J. J.; Xu, Y. P. *J. Solid State Chem.* **2007**, *180*, 1470. (b) Pan, S. L.; Smit, J. P.; Marvel, M. R.; Stern, C. L.; Watkins, B.; Poepelmeier, K. R. *Mater. Res. Bull.* **2006**, *41*, 916. (c) Pan, S. L.; Watkins, B.; Smit, J. P.; Marvel, M. R.; Saratovsky, I.; Poepelmeier, K. R. *Inorg. Chem.* **2007**, *46*, 3851.

(20) Chen, C. T.; Wu, Y. C.; Li, R. C. *J. Cryst. Growth* **1990**, *99*, 790.

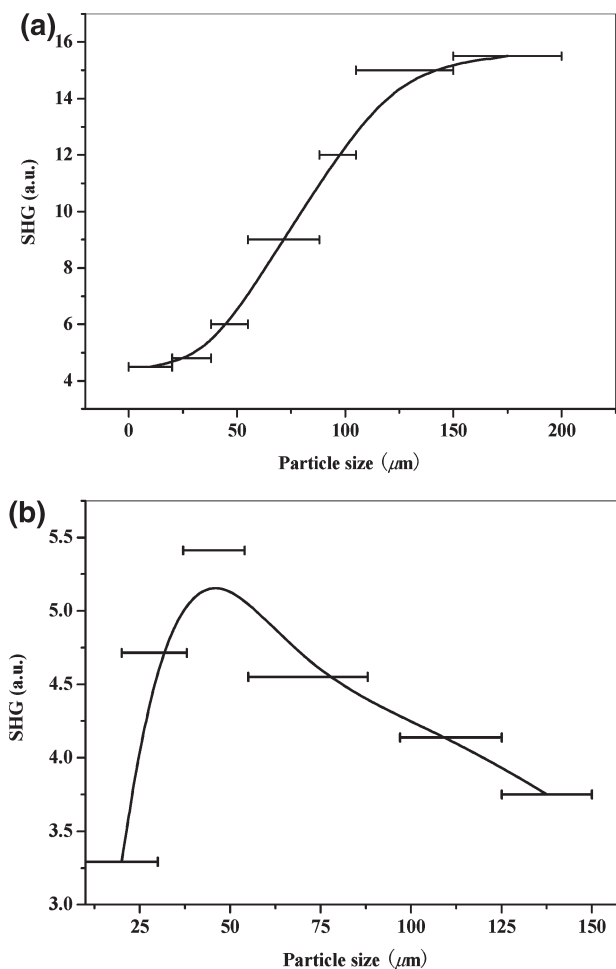


Figure 5. (a) Phase-matching curve, that is, particle size vs SHG intensity, data for $\text{Na}_2\text{B}_5\text{O}_8(\text{OH}) \cdot 2\text{H}_2\text{O}$. The curve drawn is to guide the eye and is not a fit to the data. (b) Phase matching curve, that is, particle size vs SHG intensity, data for $\text{Na}_2\text{B}_4\text{O}_5(\text{OH})_4 \cdot 3\text{H}_2\text{O}$. The curve is drawn to guide the eye and is not a fit to the data.

these show that the $\text{Na}_2\text{B}_5\text{O}_8(\text{OH}) \cdot 2\text{H}_2\text{O}$ compound is phase matchable.

For $\text{Na}_2\text{B}_4\text{O}_5(\text{OH})_4 \cdot 3\text{H}_2\text{O}$, the measurement of the SHG efficiency relative to KDP standard with the same particle size gave a value of about one-third of KDP. The powder SHG is shown in Figure 5b, showing that when the particle size is close to its coherence length, an approximately linear increase in intensity with increasing

particle size, and an inverse relation between intensity and particle size when the particle size of $\text{Na}_2\text{B}_4\text{O}_5(\text{OH})_4 \cdot 3\text{H}_2\text{O}$ becomes significantly larger than its coherence length. Furthermore, very weak green-light output was observed when 1064 nm laser permeated the crystal. All of these show that the $\text{Na}_2\text{B}_4\text{O}_5(\text{OH})_4 \cdot 3\text{H}_2\text{O}$ compound is not phase-matchable over the entire optical transmission range.

The above experiments prove that the Kurtz–Perry method has reasonably high reliability and usefulness for predicting if the materials are phase-matchable before the large single crystal are obtained.

Conclusion

In summary, $\text{Na}_2\text{B}_5\text{O}_8(\text{OH}) \cdot 2\text{H}_2\text{O}$ and $\text{Na}_2\text{B}_4\text{O}_5(\text{OH})_4 \cdot 3\text{H}_2\text{O}$ with noncentrosymmetric structure have been prepared by mild hydrothermal condition. They exhibit the SHG efficiency of about half and one-third that of KDP, respectively, and the $\text{Na}_2\text{B}_5\text{O}_8(\text{OH}) \cdot 2\text{H}_2\text{O}$ compound is phase-matchable, whereas the $\text{Na}_2\text{B}_4\text{O}_5(\text{OH})_4 \cdot 3\text{H}_2\text{O}$ compound is not.

Our studies indicate that by the introduction of the alkali metal into the borate system, we can design new types of second order NLO materials. Our future research efforts will be devoted to the exploration of new SHG compounds by introduction of other type of alkali metal or alkali earth metal into the borates.

Acknowledgment. We gratefully acknowledge the support from the National Natural Science Foundation of China (Grant 50802110), the Natural Science Foundation of Xinjiang Uygur Autonomous Region of China (Grant 200821159), the One hundred Talents Project Foundation Program, the Western Light Joint Scholar foundation program of Chinese Academy of Sciences, and the High Technology Research and Development Program of Xinjiang Uygur Autonomous Region of China (Grant 200816120).

Supporting Information Available: CIF file, tables of atomic coordinates, bond lengths and valences, symmetry transformations, crystal data and structure refinement, bond angles, and figures of powder X-ray diffraction, optical transmission spectra, and a photograph of the $\text{Na}_2\text{B}_4\text{O}_5(\text{OH})_4 \cdot 3\text{H}_2\text{O}$ crystal. This material is available free of charge via the Internet at <http://pubs.acs.org>.